

2. Palmer Station (04/05/19 – 06/30/20)

This sections describes quality control of solar data recorded at Palmer Station between 04/05/19 and 06/30/20. This period resulted in a total of 19,036 solar scans, which were assigned to Volume 29. There was a site visit at the beginning of the reporting period. Unfortunately, the system suffered from communication problems between the system's computer and the "Spectralink" subsystem that controls the monochromator. As a consequence, the wavelength position of the monochromator was frequently lost, resulting in significant data gaps (Section 2.4). The cause of this problem is still under investigation but is likely related to the upgrade of the system's operating system from Windows 7 to Windows 10 during the 2019 site visit in accordance with new cyber-security standards by NSF and NOAA. It is possible that the driver for the computer's communication card that controls peripheral system components is not reliable under Windows 10. Furthermore, the internal lamp was unstable during several "response" scans. It is not clear whether the cause of this instability was the lamp itself or a poor connection between the lamp's posts and its socket. Affected response scans were not used for processing of solar data and the problem has no impact on the quality of solar measurements.

The system's PSP radiometer was unit 30450F3 and has a calibration factor of $8.885 \times 10^{-6} \text{ V}/(\text{W m}^{-2})$, which was established on 11/1/17.

2.1. Irradiance Calibration

On-site standards

The on-site irradiance standards for the reporting period were the lamps 200W007, M700, M765, 200WN009, and 200WN010. Lamps 200WN009, and 200WN010 are "long-term" standards, which were left at Palmer Station during the March 2014 site visit. It is the intent to run lamp 200WN009 once per year to compare with the other on-site standards. 200WN010 is run every other year during site visits when all on-site lamps and the traveling standard are compared with each other. Both long-term standards were run during the 2019 site visit, and the comparison with the other lamps is discussed below.

The long-term standards 200WN009 and 200WN010 were calibrated on 12/20/2013 against lamps 200WN001 and 200WN002 using the same procedure as applied to the traveling standard 200WN014 (see below).

The working standards 200W007, M700, M765 had been recalibrated during the preparation of the previous data volume (Volume 28). The same calibrations were also used for data of the reporting period (Volume 29).

Traveling standard traceability

The traveling standard used during the site visit was lamp 200WN014. The lamp had originally been calibrated on 1/13/16 by NOAA/CUCF against lamps 200WN001 and 200WN002. Lamps 200WN001 and 200WN002 had in turn been calibrated by Biospherical Instruments in November 2012 against the NIST standard F-616 using a multi-filter transfer radiometer. NIST standard F-616 is traceable to the detector-based scale of irradiance established by NIST in 2000. At the time lamps 200WN001 and 200WN002 were calibrated, they were also compared with the long-term traveling standard 200W017 of the NSF UV monitoring network. The irradiance scales of NIST standard F-616 and lamp 200W017 agreed to within 0.3%.

The traveling standard 200WN014 was recalibrated by CUCF against lamp 200WN002 on 7/3/19. The new scale of the spectral irradiance agrees to within $\pm 0.2\%$ ($\pm 1\sigma$) with the original scale established on 1/13/16, confirming that the brightness of the lamp remains essentially unchanged. The new scale of the standard was used for the comparison shown in Fig. 1.

In early 2020, the chain of calibrations applied between 1996 and 2019 to solar data of the NSF and NOAA monitoring networks was re-evaluated. This analysis suggested that the scale of spectral irradiance of NIST standard F-616 is low compared to the scale of primary standards used before 2013. This bias ranges between -2% at 300 nm, -1% at 375 nm, and less than $\pm 0.5\%$ between 420 and 600 nm. **Version 2 solar data of Volume 29 were scaled upward accordingly, however, Version 0 remain traceable to the original scale of the primary standard F-616.**

Figure 1 shows a comparison of all lamps performed on 3/25/19, at the start of the site visit in 2019. The scales of spectral irradiance of all lamps agree to within $\pm 0.6\%$.

Lamps 200W007, M700, and M765 were also compared with each other on 7/2/19 and 12/17/19. The scales of the three lamps agreed to within $\pm 0.5\%$ on both occasions. Lamp M700 became somewhat unstable after December 2019 and “absolute” scans of this lamp were not used for the processing of solar data recorded in 2020.

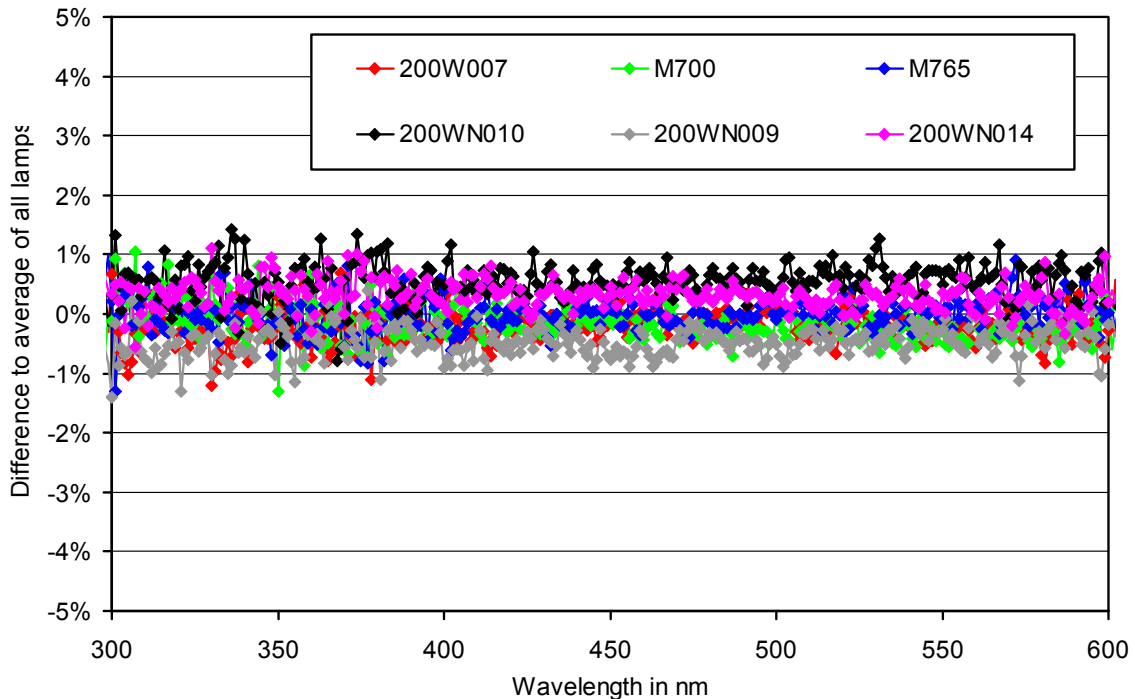


Figure 1. Comparison of the calibration of on-site standards 200W007, M700, and M765 with long-term standards 200WN009 and 200WN010, and the traveling standard 200WN014 on 3/25/2019.

To confirm the irradiance scale of solar measurements of the SUV-100 spectroradiometer chosen for the reporting period, the GU-511 radiometer that is collocated with the SUV was vicariously calibrated against SUV measurements. Calibration factors calculated with this method were compared with similar factors established during previous years. The analysis showed that calibration factors for the GU 305, 340, 380, and PAR channels that were calculated between 2013 and 2020 are in agreement to within $\pm 1.5\%$ ($\pm 2\sigma$). This result confirms the excellent consistency of SUV calibrations over time. (Of note, the change of the GU channel at 320 nm is larger than the change of the other channels because of a known drift of the 320 nm channel.)

2.2. Instrument Stability

The radiometric stability of the SUV-100 spectroradiometer was monitored with calibrations utilizing the on-site irradiance standards, with daily “response” scans of the internal lamp, by comparison with measurements of the collocated GUV-511 multifilter radiometer, and by comparisons with results of a radiative transfer model (part of “Version 2” data, see Bernhard et al. (2004)).

Error! Reference source not found. shows results from measurements of the internal lamp. Specifically, readings of the instrument’s TSI sensor (a filtered photo diode with sensitivity mostly in the UV-A) are compared with measurements of the SUV-100’s PMT at 300 and 400 nm, derived from response scans performed between 4/2/19 and 6/30/20. TSI measurements decreased by about 5% during this period, indicating that the response lamp became darker by this amount. PMT currents decreased by about the same amount. Apart from this gradual drift, about ten response scans of the reporting period had low TSI and PMT readings. The problem could have been caused by instability of the response lamp or by poor electrical contact between the lamp and its socket. Associated response scans were not used for processing of solar data.

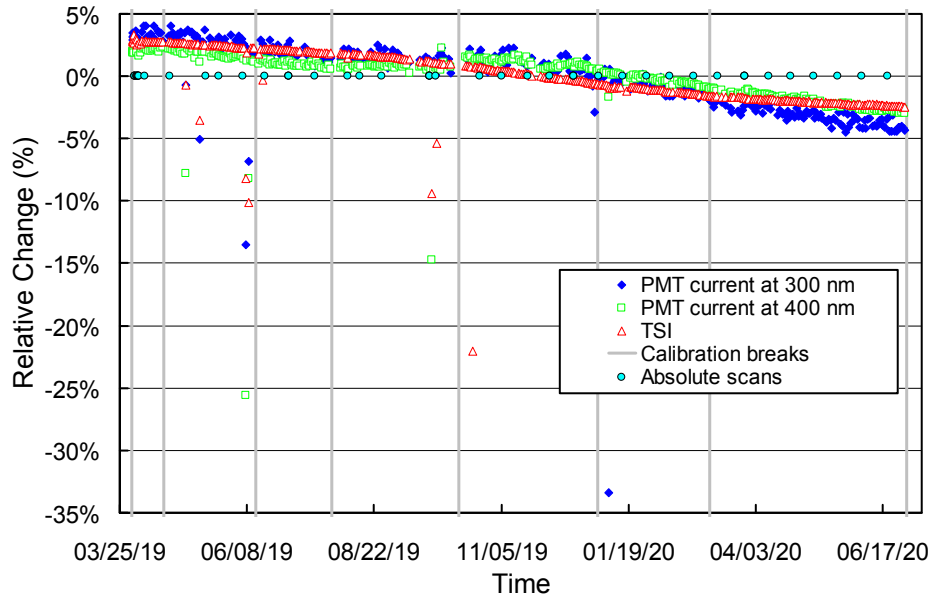


Figure 2. Time-series of PMT current at 300 and 400 nm, and TSI signal. All data were extracted from measurements of the internal irradiance standard and are normalized to their average. Calibration break points (Table 1) and times of absolute scans are also indicated.

The reporting period was divided into seven calibration periods, labeled P1 – P7 (Table 1). Figure 3 shows ratios of the calibration functions applied during Periods P1 through P7 relative to the function of Period P1. The shape of the responsivity function changed abruptly between Period P4 and P5 for reasons not understood.

Table 1. Calibration periods for Palmer Volumes 29.

Period name	Period range	Number of absolute scans
P1	04/01/19 – 04/19/19	13
P2	04/20/19 – 06/12/19	3
P3	06/13/19 – 07/27/19	4
P4	07/28/19 – 10/10/19	6
P5	10/11/19 – 12/31/19	6
P6	01/01/20 – 03/06/20	2

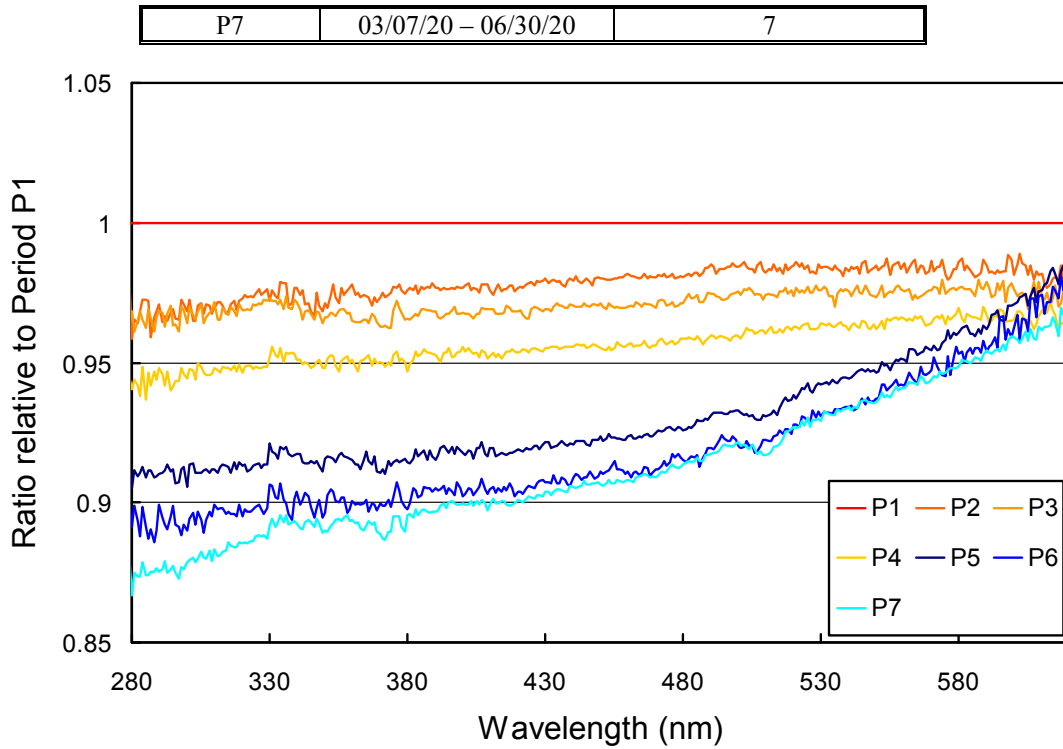


Figure 3. Ratios of spectral irradiance assigned to the internal reference lamp for periods P1 – P7, relative to Period P1.

The appropriateness of the selected calibration break points was checked by comparing calibrated SUV-100 measurements with GUV data. Figure 4 shows the ratio of GUV-511 data (340 nm channel) and final SUV-100 measurements, which were weighted with the spectral response function of this channel. The ratio is normalized and should ideally be one. There are no obvious step-changes at times of calibration breaks (green vertical lines), indicating that solar data of the SUV-100 have been appropriately corrected. GUV and SUV measurements typically agree to within $\pm 5\%$. However, Figure 4 also shows a few short periods when the ratio is abnormally high (e.g., on 4/29/19, 5/19/19, 7/22/19, 7/27/19, 8/30/19, 10/28/19, 11/13/19 – 11/17/19, and 11/19/19). On these days, snow was likely covering the irradiance collector of the SUV-100 spectroradiometer for short periods. GUV measurements are less affected by snow because the instrument is heated to a higher temperature. Hence, the ratio of GUV and SUV measurements is high after heavy snowfall until the SUV collector is again free of snow. When disregarding periods affected by snow, GUV and SUV are consistent to within $\pm 2.2\%$ ($\pm 1\sigma$). SUV measurements influenced by snow are part of the Version 0 and 2 datasets, but have been flagged in the Version 2 dataset.

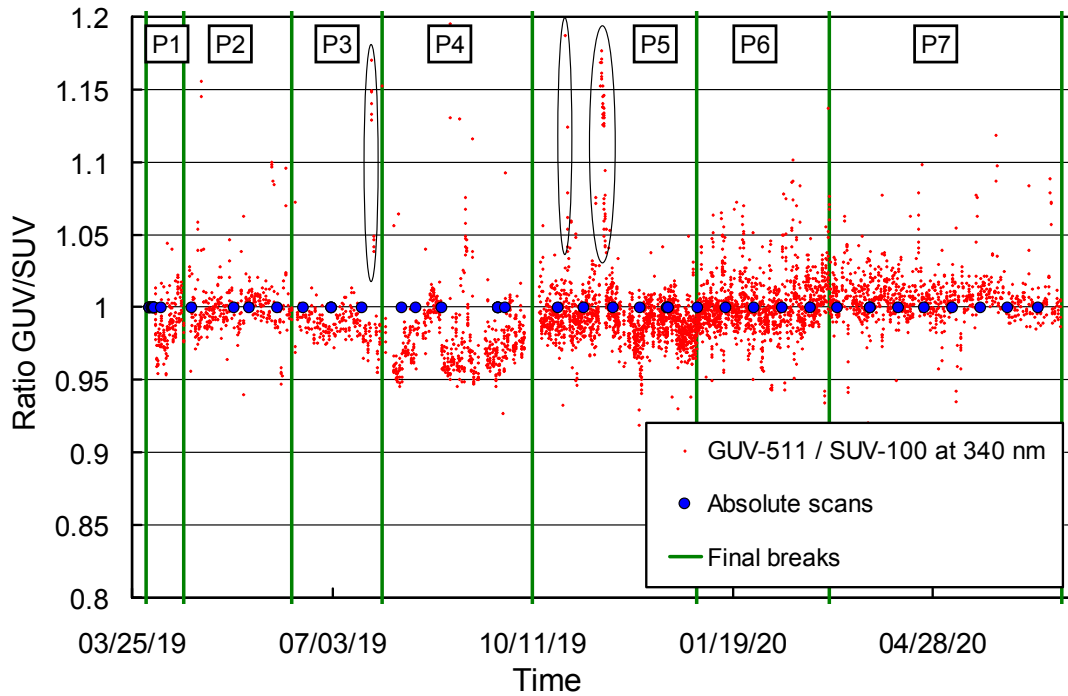


Figure 4. Ratio of GUV-511 measurements at 340 nm with final SUV-100 measurements. The latter were weighted with the spectral response function of the GUV-511's 340 nm channel. Narrow clusters of vertical data points marked by ellipses are caused by snow covering the SUV-100 collector.

2.3. Wavelength Calibration

Wavelength stability of the system was monitored with the internal mercury lamp. Information from the daily wavelength scans was used to homogenize the data set by correcting day-to-day fluctuations in the wavelength offset. The wavelength-dependent bias of this homogenized dataset and the correct wavelength scale was determined with the Version 2 Fraunhofer-line correlation method (Bernhard et al., 2004). Figure 5 shows the correction function calculated with this algorithm. Figure 6 indicates the wavelength accuracy of final Version 0 data for five wavelengths in the UV and visible by running the Version 2 Fraunhofer-line correlation method a second time. Shifts are typically smaller than ± 0.1 nm. (The standard deviations for wavelengths between 305 and 400 nm are 0.030 nm on average). There are many small steps in this time series because the system's monochromator frequently lost its wavelength position due to the communication problem between the computer and Spectralink module mentioned in the introduction. The wavelength accuracy was further improved as part of the production of Version 2 data. Figure 7 shows the wavelength accuracy of Version 2 data. There are virtually no step-changes and the standard deviations for wavelengths between 305 and 400 nm decreased to 0.019 nm.

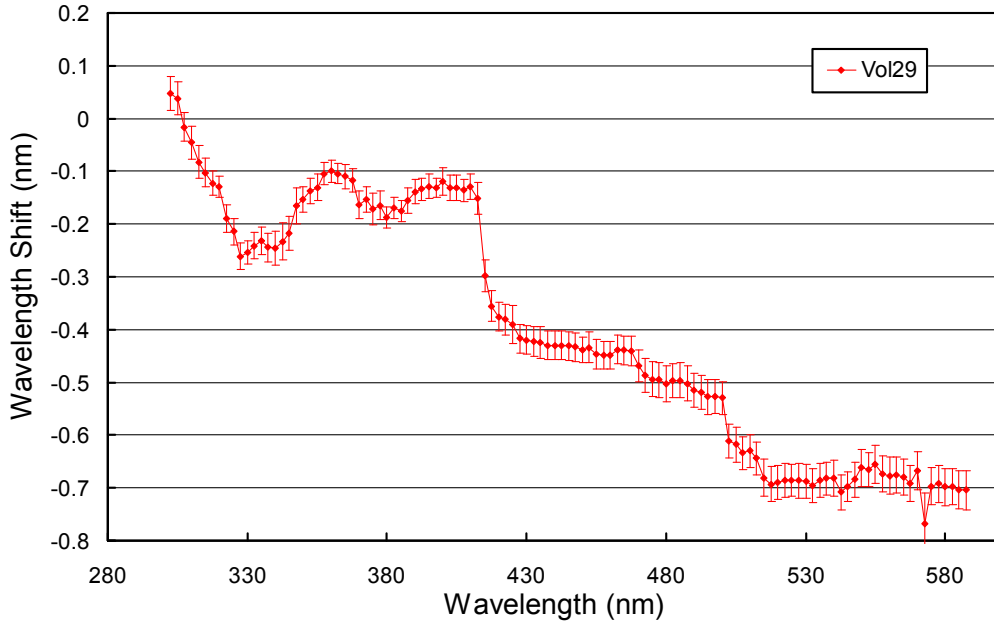


Figure 5. Monochromator mapping function. Error bars indicate 1- σ variation.

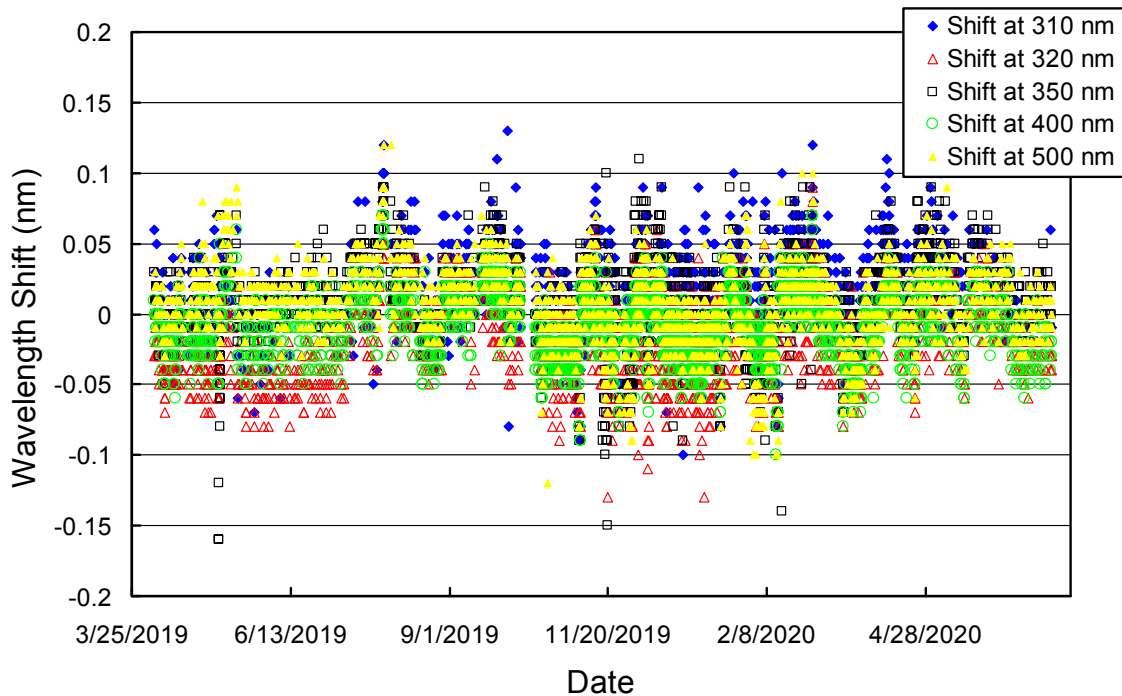


Figure 6. Wavelength accuracy check of the final Version 0 data at five wavelengths by means of Fraunhofer-line correlation. Measurements were evaluated in four-hour increments.

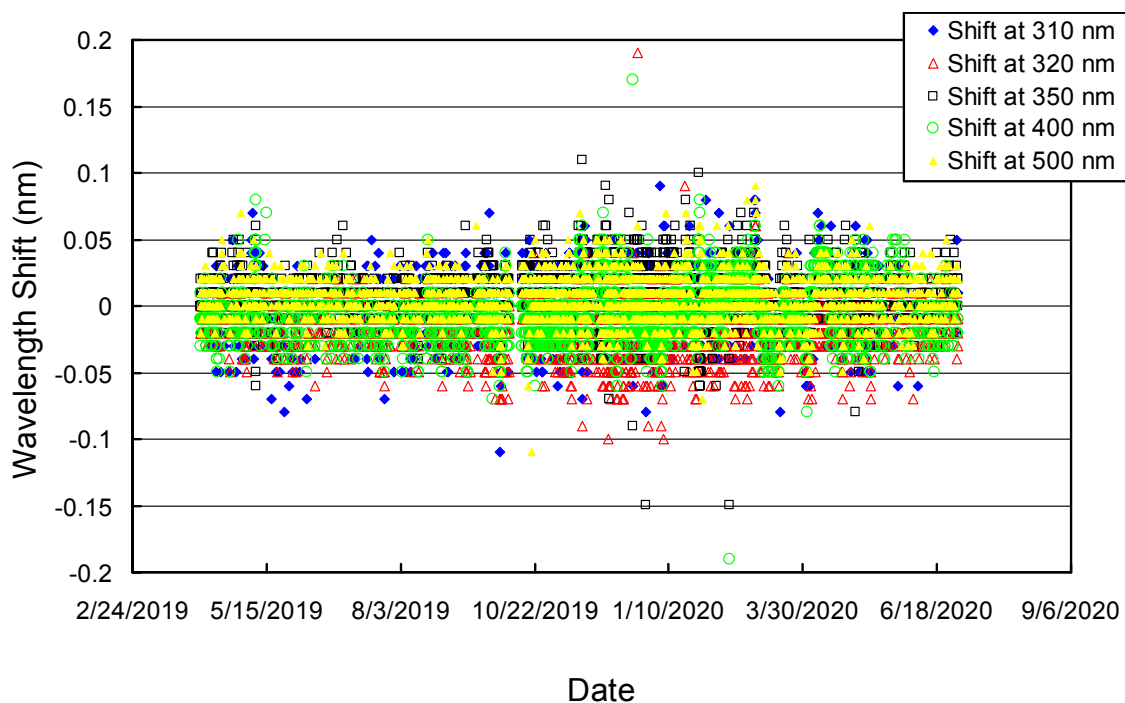


Figure 7. Same as Figure 6 but for *Version 2* data.

2.4. Missing data

Table 2 provides a list of days with missing data and indicates the cause of data gaps.

Table 2. Days with substantial data gaps.

Date	Reason
4/21/19 – 4/22/19	Communication problem Spectralink – Computer
5/15/19	No raw data
6/13/19	No raw data
7/10/19	No raw data
7/17/19	Communication problem Spectralink – Computer
7/28/19	Communication problem Spectralink – Computer
7/30/19 – 8/1/19	No raw data
8/15/19 – 8/16/19	No raw data
9/14/19 – 9/16/19	No raw data
10/3/19	No raw data
10/7/19 – 10/13/19	No raw data
11/24/19	Communication problem Spectralink – Computer
11/26/19	No raw data
12/11/19	No raw data
3/12/20	No raw data

References

Bernhard, G., C. R. Booth, and J. C. Ehamjian. (2004). Version 2 data of the National Science Foundation's Ultraviolet Radiation Monitoring Network: South Pole, *J. Geophys. Res.*, 109, D21207, doi:10.1029/2004JD004937.